Intermediate-range order in permanently densified vitreous SiO_2: A neutron-diffraction and molecular-dynamics study

S. Susman, K. J. Volin, D. L. Price, M. Grimsditch, J. P. Rino,* R. K. Kalia, and P. Vashishta
Materials Science Division, Argonne National Laboratory, Argonne, Illinois 60439

G. Gwanmesia, Y. Wang, and R. C. Liebermann
Mineral Physics Institute, State University of New York, Stony Brook, New York 11794
(Received 27 August 1990)

The structure of pressure-densified vitreous SiO_2 has been investigated using neutron-diffraction and molecular-dynamics techniques. After compression to 16 GPa at room temperature, recovered samples have densities 20% higher than normal vitreous SiO_2 and show substantial changes in the first sharp diffraction peak (FSDP): an indication of modification in the intermediate-range order. The changes in the FSDP are due to increased frustration caused by the decrease in the Si—O—Si bond angle and a shift in the Si-Si and O-O correlations in the range of 4–8 Å toward lower distances.

The irreversible densification of vitreous (amorphous) silicon dioxide (a-SiO_2) subjected to pressures above 12 GPa has been known for decades.[1–11] However, recently it has become evident that the highly densified forms of a-SiO_2 may have a very different microscopic structure than that of the "as-prepared" material and they have been termed "amorphous polymorphs". Although Raman spectroscopy shows that the microscopic arrangement of the atoms is radically changed in the densified material,[12–15] almost no structural information is available. The reason for this is that neutron scattering, which is the most powerful tool in the study of the structure of amorphous materials, cannot be applied to the small samples of densified material which are usually produced in high-pressure experiments using diamond-anvil cells. Information obtained with x rays,[13,16] which cover a much smaller range of wave vectors, has had limited success in unraveling the structure.

In this paper, we report the results of a combined neutron-diffraction and molecular-dynamics (MD) study of the structural changes which occur in permanently densified a-SiO_2 synthesized in a large-volume, high-pressure apparatus. The static structure factor of densified and normal a-SiO_2 determined by neutron diffraction are in good agreement with those obtained in the MD calculations. Both experiment and MD simulations show that there is no appreciable change in the short-range order (SRO), viz. the $Si(O_{1/2})_4$ tetrahedra, but there is a significant effect on the first sharp diffraction peak (FSDP)—the fingerprint of intermediate-range order.

The densified samples were produced at the Stony Brook High Pressure Laboratory compressing rods of normal a-SiO_2 in a uniaxial split-sphere apparatus (USSA-2000) up to pressures of 16 GPa at room temperature in 10-mm edge length MgO octahedra.[17,18] A total of four densified SiO_2 rods ~4 mm in diameter and 7–13 mm long were produced with total weight 0.943 g. Brillouin scattering was used to ascertain that the densification was the same in all the rods; the density inhomogeneities in a single rod were estimated to be 3% and within this spread all rods were equivalent. Macroscopic density measurements yielded 2.67 g/cm^3 indicating a 20% increase over that of the undensified rods.

Neutron-diffraction experiments were carried out on the Special Environment Powder Diffractometer at the Intense Pulsed Neutron Source at Argonne National Laboratory on both densified and normal a-SiO_2 obtained from the same source. Time-of-flight data were collected in six groups of time-focused detectors placed at scattering angles of $\pm 90°$, $\pm 60°$, $-30°$, and $+15°$ with respect to the incident beam. The agreement in the overlap regions between data collected with different detector banks shows that the results are not due to an experimental artifact. These data were combined by weighting with the incident neutron spectrum over the range $\lambda = 0.3$–4.0 Å. Both the densified and undensified cylindrical samples were mounted within thin-walled vanadium tubes 0.5 cm in diameter by 5 cm long. Corrections were made for container scattering, beam attenuation by sample and container, multiple scattering, and inelastic effects.[19] The detectors were normalized by means of a separate run with a vanadium standard.

Molecular-dynamics calculations were performed with effective interparticle potentials consisting of two- and three-body covalent interactions. Similar effective interactions were used previously to successfully describe the structural properties of molten and vitreous $GeSe_2$.[20,21] In the case of vitreous $GeSe_2$, the MD results for the phonon density of states (DOS) are also in good agreement with those obtained from inelastic neutron-scattering measurements.[22] Using the same interatomic-interaction scheme, we have also performed MD simulations for molten and vitreous $SiSe_2$.[23] Again the MD results for the structure and phonon DOS are in good agreement with neutron-scattering experiments.[24]

Details of the two- and three-body potentials used for a-SiO_2 are described in Ref. 25. The two-body interactions comprise Coulomb interactions due to charge transfer between Si and O, steric repulsion due to the

finite sizes of Si and O, and charge-dipole interactions to include electronic polarizability effects. The three-body covalent interactions involve the variations of Si—O bond lengths and Si—O—Si and O—Si—O bond angles.

The present calculations were carried out for a system of 648 (216 Si+432 O) particles in a box of volume 9.788×10^{-21} cm^3 for normal a-SiO_2 and 8.161×10^{-21} cm^3 in the case of densified a-SiO_2. Periodic boundary conditions were used and the long-range Coulomb interaction was treated with Ewald's summation. A time step of 0.5×10^{-15} sec was used in the Beeman[26] algorithm with the total energy conserved to 1 part in 10^4 over several thousand time steps.

In the MD studies, a-SiO_2 at normal density was obtained as follows: starting with a melt thermalized for 60 000 time steps at 3000 K, the system was cooled to 2500 K and thermalized for 30 000 time steps, then further cooled to 2000 K and thermalized for another 30 000 time steps. The melt at 2000 K was quenched at a rate of 0.1% every 10 time steps until it reached ~1500 K; at this point the system underwent thermal arrest. It was subsequently thermalized for 60 000 time steps. From this system glasses at 600, 300, and 10 K were obtained by cooling and thermalizing. The higher density glasses were obtained by increasing the density at 3000 K and repeating the above procedure.

Figure 1 shows the experimentally determined neutron structure factor, $S_N(q)$, of normal and densified a-SiO_2. Our results in the normal state agree well with previous reports.[27] Very little change can be seen in the range of large q. The FSDP, on the other hand, undergoes substantial changes in both position and intensity. Since features at small q correspond to a large range in r space, the observed changes are a qualitative indication that, while the short-range order is not changing appreciably, the intermediate-range order is substantially modified.

Information in r space can be obtained by performing the appropriate Fourier transform on $S_N(q)$; one such function is $T(r)$ which is related to the weighted (concentration and scattering cross section) pair distribution function $g_N(r)$ through

$$T(r)=4\pi\rho r\, g_N(r)\ , \tag{1}$$

where

$$g_N(r)=1+\frac{1}{4\pi\rho}\int_0^\infty [S_N(q)-1]\frac{q^2\sin(qr)}{qr}dq \tag{2}$$

and

$$g_N(r)=\frac{\left[\sum_{\alpha,\beta} c_\alpha b_\alpha c_\beta b_\beta g_{\alpha\beta}(r)\right]}{\left[\sum_\alpha c_\alpha b_\alpha\right]^2}\ . \tag{3}$$

The result of such a transformation is shown in Fig. 2. The peaks at 1.6 and 2.6 Å can be unambiguously assigned to the Si-O and O-O distances, respectively, and, as argued in the preceding paragraph, show only nominal changes in position upon densification. Additional experimental details and peak-fit parameters are presented elsewhere (see Note added in proof).

The experimental $T(r)$ is the composite of all nearest-neighbor, next-nearest-neighbor, and higher correlations. Where there is complete separation of a peak, as in the first Si-O coordination shell, a Gaussian deconvolution procedure serves to fit the peak. This works well for the next O-O peak in undensified v-SiO_2 but fails for the permanently densified material. At 3.0 Å there is a broadening of the O-O peak and a change in the sloping background. This results in an apparent shift of the Si-Si peak to larger distances. Depending on how the background is introduced, one can obtain an increase, a decrease, or no change in position of the deconvoluted peaks. We conclude that there is no unique deconvolution of the experimental $T(r)$ for distances greater than 3.0 Å. We also point out that in the region 1.9–2.3 Å in Fig. 2, there is a small increase in $T(r)$ for the densified material; although small, this increase is larger than our estimated error. This feature could be due to a few additional Si—O bonds arising as a result of densification.

Figure 3 shows the neutron (solid circles) and MD results (solid line) for $S_N(q)$ under normal and densified conditions. In both normal and densified systems, the MD calculations for the peak positions are in very good agreement with the experimental results. In the normal system the MD results for the amplitudes of all the peaks except the FSDP are also in accord with the neutron measurements. The observed discrepancy between the simulation and experiment for the height of the FSDP is

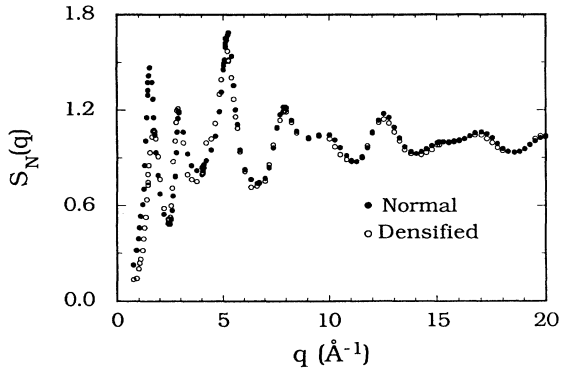

FIG. 1. Experimental results from neutron diffraction for the static structure factor $S_N(q)$ for normal and densified (20%) vitreous SiO_2.

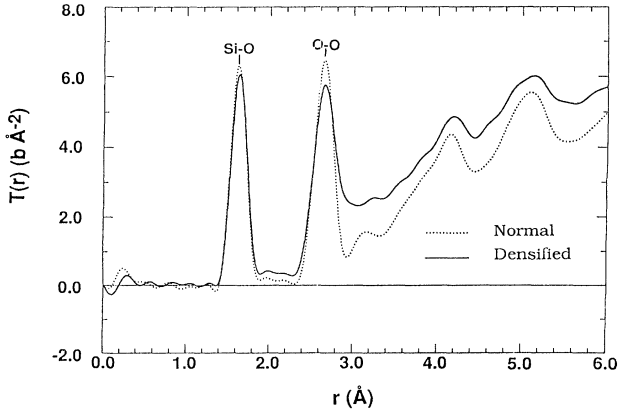

FIG. 2. $T(r)$ function from the experimental $S_N(q)$ for the normal and densified vitreous SiO_2.

a result of different quench rates used in the preparation of the computer glass and the real system.[28]

After densification, all high-q peaks remain unchanged while the FSDP shifts to larger q. The MD simulations also reveal that the amplitude of the first peak decreases on densification. These changes in the position and amplitude[29] of the FSDP are in accord with the neutron-scattering experiments. In addition, the simulation and experiment also agree on the absence of any changes in the higher-q peaks.

Molecular-dynamics results can also be used to obtain a microscopic picture of the changes occurring on densification. Figure 4 shows the MD partial pair distribution functions $g_{\alpha\beta}(r)$. In agreement with the conclusions drawn from the experimental $T(r)$ in Fig. 2, the first peaks in Si-O and O-O correlations show only minimal changes upon densification. In the region around 3.2 Å, the partial pair distribution functions show a contribution from Si-Si as well as O-O. Since $T(r)$ is weighted by concentrations and scattering lengths, the O-O contributions in this region are comparable to those of Si-Si.

On densification, the first peak in the Si-Si distribution shifts to lower distances, implying a reduction in the nearest-neighbor Si-Si distance. In all the three distributions, Si-Si, Si-O, and O-O (see insets on Fig. 4), second peaks are shifted to lower distances upon densification implying a reduction in the second-neighbor distances Si-Si2, Si-O2, and O-O2; changes in Si-Si2 are the largest and most noticeable. A slight discrepancy between experimental and MD results should be noted in the range 1.9–2.3 Å. Recall that the experimental $T(r)$ increases slightly on densification. The MD results for partial pair distribution functions do not.

Using MD configurations, microscopic structural changes upon densification can be further analyzed in terms of angular correlations between atoms. The bond-angle distributions for O—Si—O and Si—O—Si for normal and densified systems are shown in Fig. 5. In both systems the distribution of O—Si—O bond angles peaks around 109°; however, for the densified case the distribution shows broadening, signifying slight distortion of the tetrahedra at higher density. At normal density, Si—O—Si distribution shows a peak at 141° with a width (FWHM) of 26° in agreement with NMR measurements.[30] On densification the peak moves to 139° and it narrows slightly to a width of 24°. This shift in the distribution by 2° is consistent with the reduction in the Si-Si nearest-neighbor distance by 0.02 Å. Changes

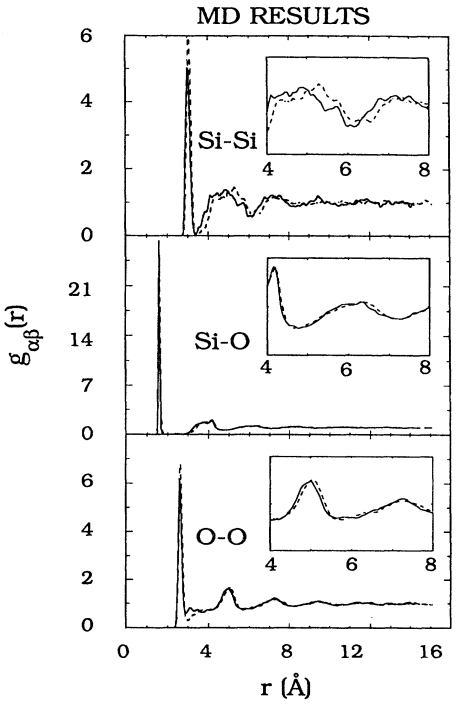

FIG. 4. MD results for partial pair distribution functions $g_{\alpha\beta}(r)$ for normal (dashed line) and densified (solid line) vitreous SiO_2. Inset shows $g_{\alpha\beta}(r)$ on an expanded scale in the range 4–8 Å.

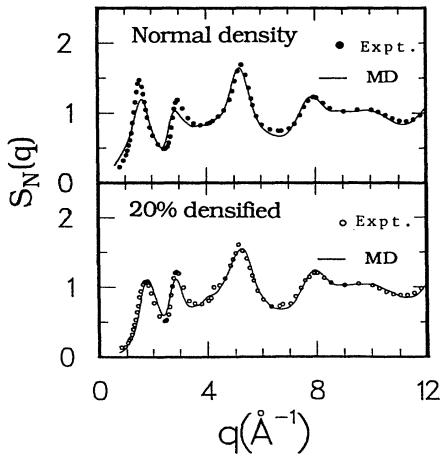

FIG. 3. Experimental and MD results for the neutron static structure factor $S_N(q)$ for normal and densified (20%) vitreous SiO_2.

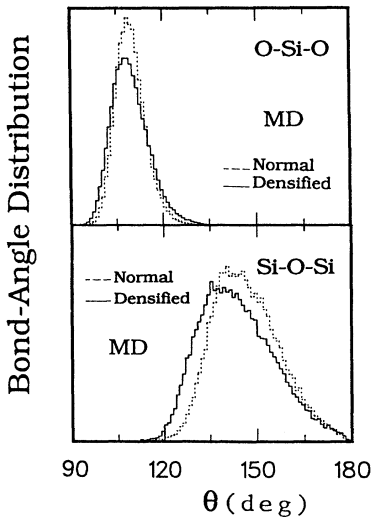

FIG. 5. Bond-angle distributions O—Si—O and Si—O—Si for normal and densified (20%) vitreous SiO_2 from MD calculations.

in other bond-angle distributions, O—O—O, O—O—Si, and Si—Si—Si (not illustrated) are also consistent: O—O—O shows a broadening of the peak at 60°, consistent with slight distortion of the $Si(O_{1/2})_4$ tetrahedra, and changes in the angles around 140° are in accord with the changes in oxygen second neighbors observed in $g_{O-O}(r)$. Changes in O—O—Si at larger angles are also in accord with the above observations. Another manifestation of the connectivity changes due to densification is the increase of the 60° peak in the Si—Si—Si bond-angle distribution. The decrease in the Si—O—Si bond angle and the shorter nearest-neighbor Si—Si distance, combined with the fact that the volume of individual $Si(O_{1/2})_4$ tetrahedra remains essentially unaltered on densification, results in the increased frustration in the packing of $Si(O_{1/2})_4$ tetrahedra. In light of the preceding analysis which provides a microscopic picture of the changes occurring upon densification, it is interesting to establish a connection between the atomic rearrangements and the observed change of the first sharp diffraction peak. As can be seen in the inset in Fig. 4, in the range 4–8 Å, the Si-O correlations do not change appreciably; however, the Si-Si and, to a lesser extent, the O-O correlations shift towards lower distances. This shift in r space moves the position of the FSDP to a larger-q value upon densification, as seen in Figs. 1 and 3. The contribution to the FSDP comes from all three correlations, Si-O, O-O, and Si-Si, and each correlation is shifted to lower distances by a different amount (the shift in Si-O being the smallest and Si-Si being the largest) resulting in broadening of the FSDP upon densification. In summary, the changes in the FSDP—shift in the position to a larger-q value, reduction in its height, and increased width—are due to increased frustration caused by the decrease in the Si—O—Si bond angle and different shifts in the Si-O, O-O, and Si-Si correlations toward lower distances in the range of 4–8 Å.

Note added in proof. An extended description of diffraction infrared and Raman studies may be found in S. Susman *et al.*, Phys. Chem. Glasses **31**, 144 (1990).

The authors are thankful to Dr. I. Ebbsjö for useful discussions and a critical reading of the manuscript. The work at Argonne National Laboratory (ANL) was supported by the U.S. Department of Energy (Division of Materials Science of the Office of Basic Energy Science), under Contract No. W-31-109-ENG-38. MD simulations were done on the Energy Research Cray Supercomputer at the National Magnetic Fusion Energy Computing Center (Livermore, CA). The work at SUNY Stony Brook High Pressure Laboratory was jointly supported by the National Science Foundation Division of Earth Sciences (Grant Nos. EAR-86-07105 and EAR-86-18830) and the State University of New York at Stony Brook. J.P.R. would like to thank the Conselho Nacional de Desenvolvimento Científico e Tecnológico (CNPq), Brazil for partial support.

*Permanent address: Universidade Federal de São Carlos, 13 560 São Carlos, São Paulo, Brazil.

[1]P. W. Bridgman and I. Simon, J. Appl. Phys. **24**, 405 (1953).
[2]E. B. Christiansen *et al.*, J. Am. Ceram. Soc. **45**, 172 (1962).
[3]R. Roy and H. M. Cohen, Nature (London) **190**, 789 (1961).
[4]J. D. Mackenzie, J. Am. Ceram. Soc. **46**, 461 (1963).
[5]S. Sakka and J. D. Mackenzie, J. Non-Cryst. Solids **1**, 107 (1969).
[6]J. Arndt and D. Stöffler, Phys. Chem. Glasses **10**, 117 (1969).
[7]J. Arndt, J. Am. Ceram. Soc. **52**, 285 (1969).
[8]R. Bruckner, J. Non-Cryst. Solids **5**, 123 (1970).
[9]A. G. Revesz, J. Non-Cryst. Solids **7**, 77 (1972).
[10]For a review see W. Primak, *The Compacted States of Vitreous Silica* (Gordon and Breach, New York, 1975).
[11]J. Arndt, Phys. Chem. Glasses **24**, 104 (1983).
[12]S. Mochizuki and N. Kawai, Solid State Commun. **11**, 763 (1972).
[13]P. McMillan *et al.*, J. Chem. Phys. **81**, 4234 (1984); R. Couty, thèse de Doctorat d'Etat, Université de Paris VI, 1977.
[14]M. Grimsditch, Phys. Rev. Lett. **52**, 2379 (1984); Phys. Rev. B **34**, 4372 (1986).
[15]R. J. Hemley *et al.*, Phys. Rev. Lett. **57**, 747 (1986).
[16]A. J. Leadbetter and A. C. Wright, Phys. Chem. Glasses **18**, 79 (1977).
[17]T. Gasparik, Contrib. Mineral. Petrol. **102**, 389 (1989); A. R. Remsberg *et al.*, Phys. Chem. Mineral. **15**, 498 (1988).
[18]The starting 4-mm-diam fused silica rod contained 295-ppmW hydroxide as measured by the 367-cm^{-1} infrared absorption band. Adjacent portions of this rod were used for the neutron-diffraction measurements on undensified and densified vitreous silica. The experimental conditions and the volumes of sample in the beam were identical in all cases.
[19]D. L. Price *et al.*, J. Non-Cryst. Solids **66**, 443 (1984).
[20]P. Vashishta *et al.*, Phys. Rev. B **39**, 6034 (1989); and P. Vashishta *et al.*, Phys. Rev. Lett. **62**, 1651 (1989).
[21]The basis for using similar effective potentials is that SiO_2 and binary chalcogenide glasses have several common structural features. These include tetrahedral units comprising short-range order and the medium-range order manifested in the form of FSDP.
[22]U. Walter *et al.*, Phys. Rev. B **37**, 4232 (1988). Even a subtle feature such as the companion line of the symmetric breathing mode is found present in the MD results. The energy of the companion line is also in accord with the Raman scattering measurements.
[23]P. Vashishta, R. K. Kalia, J. P. Rino, and I. Ebbsjö (unpublished).
[24]M. Arai *et al.*, Phys. Rev. B **37**, 4240 (1988).
[25]P. Vashishta *et al.*, Phys. Rev. B **41**, 12 197 (1990).
[26]D. Beeman, J. Comp. Phys. **20**, 130 (1976).
[27]P. A. V. Johnson *et al.*, J. Non-Cryst. Solids **58**, 109 (1983).
[28]Different quench rates do not affect the peak positions or the amplitudes of the second-, third-, and higher-order peaks in the structure factor. As regards the FSDP, its position is unaffected but its amplitude diminishes with an increase in the rate of quenching. The larger the quench rate, the higher the frustration of tetrahedral packing. This diminishes medium-range correlations, causing a decrease in the amplitude.
[29]In light of much higher quench rates in simulation, the excellent agreement on the amplitude of the FSDP may be fortuitous.
[30]R. F. Pettifer *et al.*, J. Non-Cryst. Solids **106**, 408 (1988); R. L. Mozzi and B. E. Warren, J. Appl. Cryst. **2**, 164 (1969).